

A search for counter-rotating stars in S0 galaxies

Konrad Kuijken^{1*}, David Fisher¹ and Michael R. Merrifield²

¹ *Kapteyn Astronomical Institute, University of Groningen, P.O. Box 800, 9700 AV Groningen, The Netherlands*

² *Department of Physics, University of Southampton, Highfield SO9 5NH, UK*

19 September 2018

ABSTRACT

We have obtained high signal-to-noise spectra along the major axes of 28 S0 galaxies in order to search for the presence of disk stars on retrograde orbits. Full line-of-sight velocity distributions were extracted from the data, and the velocity distributions were modelled as arising from the superposition of populations of stars on prograde and retrograde orbits. We find no new cases in which a significant fraction of disk stars lie on retrograde orbits; an identical analysis of NGC 4550 does reveal the previously-known counter-rotating stellar disk in this system. Upper limits determined for each object indicate that no more than $\sim 5\%$ of the observed disk star light could arise from counter-rotating stellar components. These results suggest that previously-discovered disk galaxies with counter-rotating stars are exceptional and that (at 95% confidence) at most 10% of S0 galaxies contain significant counter-rotating populations. The most likely value for the fraction of such S0 galaxies lies closer to 1%. This result contrasts with the prevalence of counter-rotating gas in these systems; combining our new observations with existing data, we find that $24 \pm 8\%$ ($1\text{-}\sigma$ error) of the gas disks in S0 galaxies counter-rotate relative to their stellar components.

Key words: line: profiles – galaxies: elliptical and lenticular, cD – galaxies: kinematics and dynamics – galaxies: structure

1 INTRODUCTION

Over recent years, a number of techniques have been developed which use high signal-to-noise ratio spectra of galaxies to obtain detailed information as to their stellar kinematics (eg Bender 1990; Rix and White 1992; van der Marel and Franx 1993; Gerhard 1993; Kuijken and Merrifield 1993; Saha & Williams 1994; Statler 1995). These techniques, in combination with photometric measurements, have provided new insights into the properties of a variety of galaxy components, including nuclear disks (van der Marel et al. 1994), the outskirts of elliptical galaxies (Bender, Saglia & Gerhard 1994; Carollo et al. 1995), peanut-shaped bulges (Kuijken & Merrifield 1995), and bars (Merrifield & Kuijken 1995).

However, perhaps the most dramatic discovery has been the detection of disk galaxies in which a significant fraction of the stars are on retrograde orbits. Such a counter-rotating population was first discovered by Rubin et al. (1992) in the Virgo lenticular NGC 4550. This system was found to contain a disk in which half of the stars circulate in one direction while the other half orbit in the opposite direction (Rix et al. 1992). The only other documented example of a large-scale counter-rotating stellar disk is in the Sab galaxy NGC 7217,

in which Merrifield & Kuijken (1994) discovered that the disk is made up from two distinct components with approximately two-thirds on prograde orbits and one-third on retrograde orbits. This smaller retrograde population only showed up after a careful analysis of the line-of-sight velocity distribution (LOSVD) derived from absorption-line spectra at a number of radii in the system: disk stars in the main prograde component follow approximately circular orbits, and so produce large peaks in the observed LOSVDs at the projected circular speed of the galaxy (relative to its systemic velocity); the counter-rotating population shows up in the complete velocity distributions as secondary peaks at close to minus the projected circular velocity.

One possibly-related phenomenon is the relatively high frequency with which gas disks in early-type disk galaxies are observed to counter-rotate. Bertola et al. (1992) find that approximately 20% of the gas disks found in S0 galaxies rotate in the opposite direction to the stars in these systems. There is no *a priori* reason to suppose that stars cannot form in such gas just as they do in gas on more normal prograde orbits, and so we might expect counter-rotating stellar populations to form in these systems. However, the gas disks in these early-type galaxies are usually restricted to their cores, and so any counter-rotating stars that they produce are likely to be in a similar small region. Support for this scenario has come from recent observations

* Visiting Scientist, Dept. of Theoretical Physics, University of the Basque Country, Bilbao, Spain

of the Sa galaxy NGC 3593, which has been found to contain both a counter-rotating gas disk in its core and a counter-rotating stellar disk on a similar small spatial scale (Bertola et al. 1996). Similarly, Prada et al. (1996) have found that there is a counter-rotating stellar component in the bulge region of the Sb galaxy NGC 7331. Although star formation in central counter-rotating gas disks could result in these relatively small-scale phenomena, it could not produce the large-scale counter-rotating stellar populations that we see in NGC 4550 and NGC 7217, and it is not clear how closely these two phenomena are related.

One problem in trying to interpret large-scale stellar counter-rotation is that only a very small number of disk galaxies have been subjected to the sort of detailed kinematic analysis required to detect modest fractions of stars on retrograde orbits. The possibility therefore exists that such counter-rotating populations could lie undetected in a significant percentage of all disk galaxies. Further, it is difficult to make a statistical interpretation of the existing data: most of the known cases of counter-rotation (both stellar and gaseous) were detected serendipitously, and this rather heterogeneous data set lacks well-defined selection criteria.

We have therefore obtained high signal-to-noise ratio spectra for a well-defined sample of 28 early-type disk galaxies. In this paper, we present the kinematic analysis of these data, and use them to calculate the frequency of both stellar and gaseous counter-rotation in such systems.

2 DATA REDUCTION AND ANALYSIS

The galaxies chosen for this study (see Table 1) were selected from the Third Reference Catalogue of Bright Galaxies (de Vaucouleurs et al. 1991). They belong to Hubble morphological types S0, SB0, and SA0, which hereafter will be collectively referred to as S0 galaxies. The sample consists of objects in a variety of environments, with members drawn from the field, small groups and rich clusters. We restricted our sample of disk galaxies to early-types because their smooth light profiles and comparatively uniform stellar populations enable accurate measures of the stellar kinematics. This selection also has the benefit that the possible complicating influences on measurement and interpretation from gas, dust, and star forming regions are minimized compared to later-type spirals. Furthermore, it has been argued that the frequency of counter-rotating stars might be higher in earlier-type disk galaxies (Merrifield & Kuijken 1994). In order to maximize the projection into the line of sight of the stellar rotational motion (and hence maximize the characteristic signal from any counter-rotating population), preference was given to observing edge-on objects. Apart from NGC 3998 (inclination 35°), all galaxies in our sample have inclinations of at least 50° , with more than half inclined more than 80° . Of the sample galaxies, only NGC 4550 was known to exhibit counterrotating stars when this project was started.

The spectra analyzed here were obtained with the Shane Telescope through the KAST spectrograph at Lick Observatory, and the Multiple Mirror Telescope at Mount Hopkins, using the Red Channel Spectrograph. The Lick observations were taken through a $2 \text{ arcsec} \times 2.6 \text{ arcmin}$ slit with a $1200 \text{ line mm}^{-1}$ grating, resulting in a spectral resolution

Table 1. Parameters for the galaxy sample observed

| Galaxy | B_T° | Type | PA _{maj} | Obs | Gas |
|-----------|-------------|------------------|-------------------|-----|-----|
| NGC 128 | 12.66 | S0 pec | 1 | M | – |
| NGC 1184 | 13.44 | S0/a | 167 | M | + |
| NGC 1332 | 11.25 | S0 [–] | 148 | M | |
| NGC 1461 | 12.66 | SA0 ^o | 155 | L | |
| NGC 1611 | 12.95 | SB0 ⁺ | 77 | M | + |
| NGC 2549 | 12.04 | SA0 ^o | 177 | M | |
| NGC 2560 | 14.08 | S0/a | 93 | L | |
| NGC 2612 | 13.5 | S0 [–] | 115 | M | – |
| NGC 3098 | 13.00 | S0 | 90 | M | + |
| NGC 3115 | 9.75 | S0 [–] | 43 | L | |
| NGC 3384 | 10.75 | SB0 [–] | 53 | L | |
| NGC 3412 | 11.35 | SB0 ^o | 155 | L | |
| NGC 3607 | 10.87 | SA0 ^o | 120 | L | + |
| NGC 3941 | 11.27 | SB0 ^o | 10 | L | – |
| NGC 3998 | 11.54 | SA0 ^o | 140 | L | + |
| NGC 4026 | 11.60 | S0 | 178 | L | + |
| NGC 4036 | 11.52 | S0 [–] | 85 | L | + |
| NGC 4111 | 11.62 | SA0 ⁺ | 150 | L,M | + |
| NGC 4124 | 12.12 | SA0 ⁺ | 114 | M | + |
| NGC 4179 | 11.97 | S0 | 143 | M | + |
| NGC 4251 | 11.54 | SB0 | 100 | L | |
| NGC 4350 | 11.87 | SA0 | 28 | L | + |
| NGC 4550† | 12.4 | SB0 | 178 | L | |
| NGC 4710 | 11.84 | SA0 ⁺ | 27 | M | |
| NGC 4754 | 11.38 | SB0 [–] | 23 | L | |
| NGC 4762 | 11.05 | SB0 ^o | 32 | L | + |
| NGC 5308 | 12.43 | S0 [–] | 60 | M | |
| NGC 5866 | 10.87 | SA0 ⁺ | 128 | L | + |
| NGC 7332 | 11.96 | S0 | 155 | M | – |

Total B band ‘face-on’ magnitudes, B_T° , corrected for Galactic and internal extinction, and for redshift from RC3 (de Vaucouleurs et al. 1991). For NGC 1184 we give m_B and for NGC 1611 we give m_{FIR} both from the RC3. For NGC 2612 we quote the value given in the NASA Extragalactic Database. Galaxy types are as given in the RC3. Major axis position angles, PA_{maj}, are taken from the RC3 except for NGC 1184 which was determined by eye. The ‘Obs’ column denotes whether the galaxy was observed from the Lick (L) or the Multiple Mirror Telescope Observatory (M). The final column indicates whether gas was detected, and, if so, whether it follows prograde (+) or retrograde (–) orbits. †NGC 4550 was known to contain counterrotating disks before this survey was started, and is not included in the final statistics.

of 3.1 \AA (FWHM) corresponding to a instrumental dispersion of $\sigma=75 \text{ km/s}$. The MMT spectrograph was configured with a $1200 \text{ line mm}^{-1}$ grating and a $1.25 \text{ arcsec} \times 3 \text{ arcmin}$ slit giving a resolution of 2.6 \AA (instrumental $\sigma=63 \text{ km/s}$). For both sets of observations, the spectral region around the Mg b triplet at 5170 \AA was observed with integration times of typically 40 – 60 min.

The techniques employed here to determine the galaxy line profiles are the expansion of the LOSVD into a truncated Gauss-Hermite series (van der Marel and Franx 1993) and the unresolved Gaussian decomposition (UGD) method of Kuijken and Merrifield (1993). In the first method the velocity distribution is parametrised by the Gauss-Hermite series of orthogonal functions yielding two measures of the deviations of the line profile from a gaussian: a parameter h_3 which measures asymmetric deviations, and a parameter h_4 measuring symmetric deviations. The UGD method

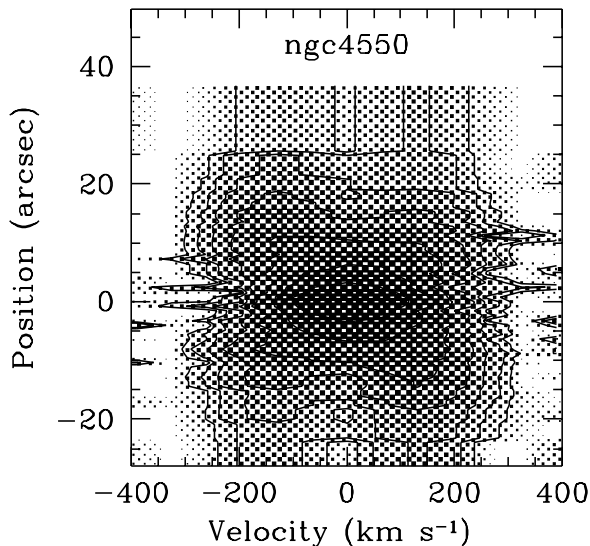


Figure 1. The line-of-sight velocity distribution for NGC 4550, as derived with the unresolved gaussian decomposition method. The greyscales and contours indicate the projected phase space density (stars $\text{arcsec}^{-1} \text{ km s}^{-1}$) on the major axis. Contours are logarithmically spaced, separated by factors of $2^{1/2}$. In agreement with the results of Rix et al. (1992), two counterrotating stellar components are clearly identifiable.

extracts the stellar LOSVD by modeling the velocity distribution produced by the Doppler broadening and velocity shift in the galaxy spectrum. The line profile is modeled as the sum of a set of unresolved (ie overlapping) gaussians with fixed means and dispersions. The optimal LOSVD is obtained by convolving the modeled LOSVD with spectra of template stars and minimizing the least-squares comparison with the galaxy spectrum by varying the amplitudes of the gaussian components.

3 RESULTS

In this section we present the LOSVDs derived using the UGD method for our sample.

As a guide to the eye, we first show the result for the galaxy NGC 4550 in which the signature of counter-rotating disks is clearly seen as a splitting of the line profile into two approximately equal strength peaks (Fig. 1). This figure demonstrates that our data and analysis technique are indeed capable of revealing counter-rotating components, in agreement with the double-gaussian analysis of this galaxy’s spectra by Rix et al. (1992).

Figure 2 displays the stellar LOSVDs for the remainder of our sample of objects as derived from the UGD method. It is apparent from Fig. 1 that NGC 4550 is unique among the galaxies in our sample as none displays a comparable LOSVD. A number of the objects (e.g., NGC 3384, NGC 4111, NGC 4762) have line profiles suggestive of independent kinematic components such as nuclear disks and bars. However, there are no obvious signs of counter-rotation.

The line profiles have been analyzed further by generating cumulative velocity distributions which indicate the fraction of stars at successive velocity increments. An example is shown in Fig. 3 for the major axis of NGC 4036. In this representative case, no peculiarities are present in the ‘rotation curve’ with the only distinguishing feature being a low-speed tail which reaches its greatest skewness at a radius of 10 arcseconds. This produces an asymmetry in the line profile resulting in h_3 terms of magnitude 0.1 as output by the Gauss-Hermite expansion. Such tails are generically expected in disks with radially decreasing density and velocity dispersions (Kuijken & Tremaine 1992); line-of-sight projection through the edge-on galaxy further enhances the skewness. For comparison, we also plot the cumulative velocity distribution for NGC 4550, which shows that roughly equal numbers of stars populate each component.

3.1 Upper limits on counter-rotating populations

A straightforward procedure for estimating the upper limit on the counter-rotating stars is as follows. Starting from the measured LOSVDs (which we will call the prograde model), we construct a retrograde model by inverting all velocities with respect to the galaxy’s systemic velocity. We then convolve both the prograde and retrograde velocity distributions with the stellar template spectrum, resulting in two model spectra: one for the prograde stars, one for the retrograde ones. We then attempt to model the observed galaxy spectrum as a linear superposition of the pro- and retrograde models, and evaluate the statistical bounds on the coefficient of the retrograde model. Only those spectra which cover the flat part of the rotation curve, outside the bulge, are included in the analysis. The upper limits obtained in this way range between 2 and 6% ($3\text{-}\sigma$).

These formal errors reflect pure photon statistics, without allowance for possible systematic errors. The most important such effect is template mismatch, which occurs when the stellar template chosen differs from the average stellar spectrum in the galaxy. In order to investigate the importance of this effect, we have derived the LOSVDs for a number of the observed galaxies using template stars with a range of spectral types. As Fig. 4 illustrates, this analysis reveals that template mismatch can produce spurious features in the derived distributions at around the 5% level. It is this effect which is probably responsible for the three galaxies (NGC 2612, NGC 3098, NGC 5866) where the LOSVDs shown in Fig. 2 are mildly suggestive of counter-rotation. Template mismatch thus makes it impossible to constrain the presence of such counter-rotating stars to a level better than 5% from the present analysis. It should also be remembered that the UGD analysis, which does not allow negative line profiles, contains a slight bias towards creating positive LOSVD peaks at the $1\text{-}\sigma$ level at velocities where there is in reality no flux.

Limits on any counterrotating disk stars in the bulge regions of the galaxies are more difficult to obtain. In these regions the background from the kinematically hot bulge is more difficult to separate from any superimposed disk, and the distinction between disk and bulge is not clear without further information about vertical kinematic gradients. We therefore do not emphasize the bulge regions in this study;

Figure 2. Velocity distributions along the major axes of the sample galaxies. Positions and radial velocities are given with respect to the centre of each galaxy. The contour levels are separated by factors of $2^{1/2}$ in density; greyscale levels jump every other contour. Features at the lowest levels in these panels may be artefacts of the particular stellar template spectrum chosen for the analysis (see text).

Figure 2 – continued

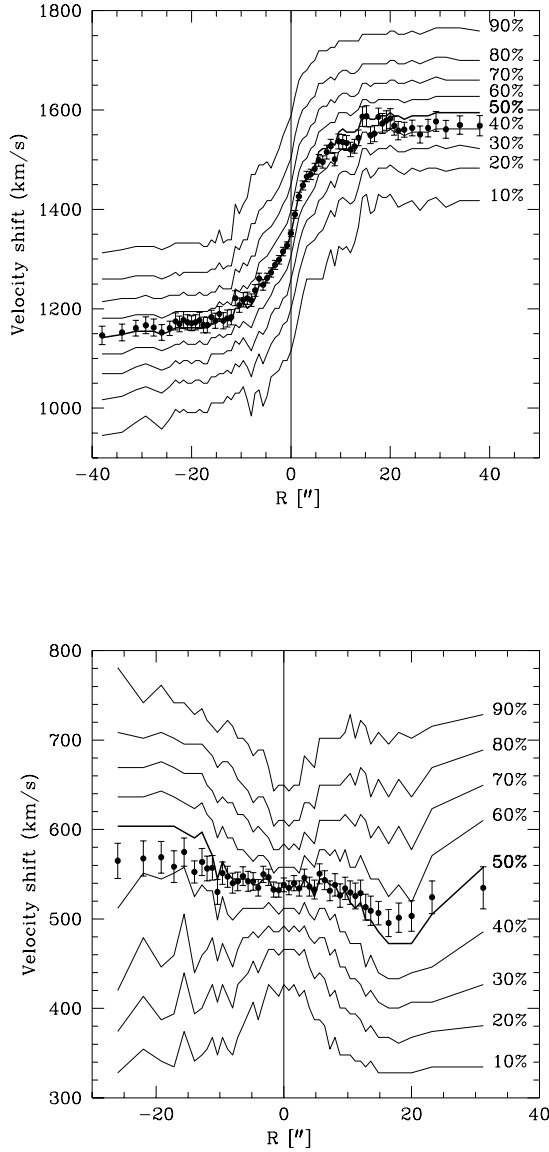


Figure 3. Contours of the cumulative velocity distributions for NGC 4036 (top) and NGC 4550 (bottom). (10% of the stars have radial velocity below the line labelled 10%, etc.) This figure illustrates the strong limits that our data can place on the fraction of counterrotating stars. Points with error bars give the mean velocity at each radius.

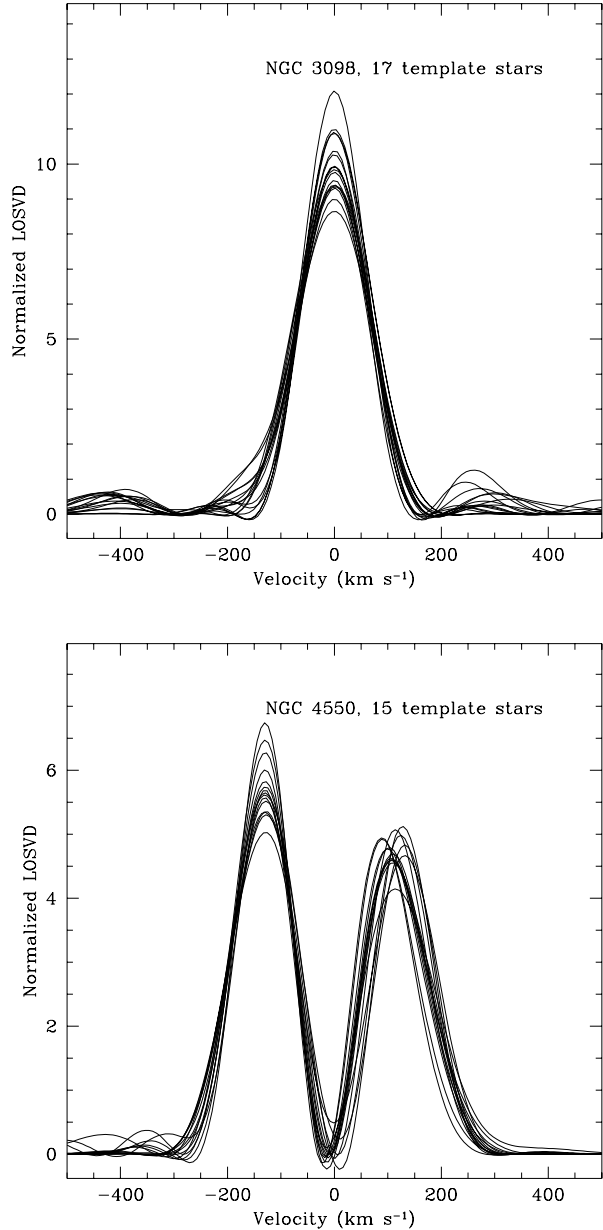


Figure 4. LOSVDs derived from a point in the disks of NGC 3098 (top) and NGC 4550 (bottom). The distributions have been derived using stellar templates with a range of spectral (F – M), and it is clear that the choice of template type affects the derived velocity distribution at around the 5% level.

at first sight, none of our sample galaxies show strong indications for counter-rotating central stellar disks.

3.2 The fraction of S0 galaxies with counter-rotating stellar disks

Given that we find no evidence for counter-rotation in our sample of 28 objects (excluding NGC 4550, which was not observed as part of our unbiased survey), what limit does our result place on the fraction p of all galaxies which can contain counter-rotating populations? Simple binomial distribution statistics show that if p were greater than 10%, the probability of not finding even one case in our sample would be less than 5%. The 95% confidence upper limit for p is thus 10%.[†]

3.3 The fraction of S0 galaxies with counter-rotating gaseous disks

Our spectral observations of these galaxies cover the 4959Å and 5007Å lines of [OIII], as well as Hβ at 4861Å. We can thus also use the data to search for emission lines in these systems, and measure the fraction in which any gas that we detect is found to be counter-rotating. Since the sample galaxies were not selected on the basis of their gaseous properties, these data provide an unbiased estimate for the fraction of S0 galaxies containing counter-rotating gas disks. The last column in Table 1 shows in which galaxies emission line gas was detected, and in which systems it follows retrograde orbits. Of the 28 galaxies in the sample, gas was detected in 17. Thirteen of these systems are prograde, while the remaining four contain gas on retrograde orbits. We thus find that the counter-rotating gas disks make up $24 \pm 10\%$ ($1-\sigma$ error; the 90% confidence interval is 8 – 46%). This value agrees very well with the figure of $\sim 20\%$ that Bertola et al. (1992) obtain from a sample of 15 S0 galaxies selected on the basis of their known extended gas emission. The two samples have three galaxies in common,[‡] and of the combined sample of 29 galaxies in which gas is detected, we find that the orbits are retrograde in 7 systems. Our best estimate for the fraction of S0 galaxy gas disks which counter-rotate relative to the stellar component is thus $24 \pm 8\%$ ($1-\sigma$ errors; 12 – 40% with 90% confidence).

4 DISCUSSION

The goal of the present study has been to search for the presence of counter-rotating stars in S0 galaxies through an analysis of their line-of-sight velocity distributions. No new

[†] It is unwise to incorporate NGC 4550 itself into these statistics, since we observed it precisely because it had been shown to contain a counter-rotating disk. However, including it with full weight in the statistics would yield a somewhat biased confidence interval of $3.5^{+13.5}_{-3.4}\%$, not dramatically different from the upper limit quoted above.

[‡] For one of the galaxies in both samples, NGC 128, we find that the gas is on retrograde orbits, in disagreement with Bertola et al.'s tabulated result. Our result is confirmed by Emsellem et al. (1995)

cases of stellar counter-rotation have been found. The upper limits derived from this analysis imply that no more than $\sim 5\%$ of the disk stars in our sample galaxies could remain undetected on retrograde orbits. This analysis implies that the previously-discovered examples of disk galaxies with counter-rotating stars are quite rare: at 95% confidence we can say that no more than 10% of S0 galaxies contain detectable counterrotating stellar disks. Successful theories of galaxy formation must, however, still take account for these unusual objects, and so it is worth discussing how these systems might have formed.

Galaxy mergers provide the most obvious mechanism by which counter-rotating populations might form. However, mergers of equal-mass disk galaxies with antiparallel spins result in systems that would not be identified as a disk galaxy – the heating of the initial galaxies is too great to preserve the disk structure (Barnes 1992). Less dramatic merging of satellites on to galaxy disks can produce counter-rotation (Thakar & Ryden 1996), but still cannot explain the equal-mass counter-rotating disks seen in NGC 4550.

A more general scenario for the formation of galaxies with counter-rotating disks is via the steady infall of gas onto a preexisting disk system (see Bettoni & Galletta 1992; Rix et al. 1992; Merrifield & Kuijken 1994). Numerical simulations by Thakar & Ryden (1996) indicate that the accretion of diffuse gas can, indeed, lead to the formation of large-scale counter-rotating components.

The prevalence of counter-rotating gaseous disks that we find in S0 galaxies provides support for a scenario of this kind. However, most of these gas disks are quite small, and cannot be responsible for large-scale counter-rotating stellar disks such as NGC 4550 or NGC 7217, but are more likely to produce centrally-concentrated retrograde stellar populations such as the one discovered in NGC 3593 (Bertola et al. 1996). The two galaxies in our sample which contain more extensive counter-rotating gas disks – NGC 3941 and NGC 7332 (Fisher 1994; Fisher, Illingworth & Franx 1994) – show no signs of corresponding counter-rotating stellar components. In the case of NGC 7332, the emission-line gas is clearly not yet relaxed, so the lack of associated stars is perhaps not a surprise. In NGC 3941 the gas disk appears well settled, with a radius of about 30 arcseconds (2.7kpc). Roberts et al. (1991) quote a total HI gas mass of $1.3 \times 10^9 M_{\odot}$ for this galaxy ($H_0 = 50 \text{ km s}^{-1} \text{ kpc}^{-1}$), which, if it all resides in the retrograde gas disk, would be responsible for about 5% of the mass in the inner 2.7 kpc – more if there is also a substantial molecular component. The absence of a counter-rotating stellar component in this system then suggests that star-formation may be inhibited in gas on retrograde orbits, possibly because of interaction with the stellar winds from the prograde stars. However, high-resolution mapping of this system in HI and CO is required before any firm conclusion can be drawn. If it does prove to be difficult to produce stars in massive retrograde gas disks, then the mystery surrounding the few rare cases which do contain large-scale counter-rotating stellar populations deepens still further.

ACKNOWLEDGEMENTS

The data presented in this paper were obtained at Lick Observatory which is operated by the University of California and with the Multiple Mirror Telescope which is a joint facility of the Smithsonian Institute and the University of Arizona. Much of the analysis was performed using IRAF, which is distributed by NOAO. MRM is supported by a PPARC Advanced Fellowship (B/94/AF/1840). We thank Marijn Franx for a careful reading of the manuscript, and the referee, Gerry Gilmore, for constructive comments.

REFERENCES

- Barnes, J. E. 1992, *ApJ*, 393, 484
 Bender, R. 1990, *A&A*, 229, 441
 Bender, R., Saglia, R. P. & Gerhard, O. E. 1994, *MNRAS*, 269, 785
 Bertola, F., Buson, L. M. & Zeilinger, W. W. 1992, *ApJ*, 401, L79
 Bertola, F., Cinzano, P., Corsini, E. Pizzella, A., Persic, M. & Salucci, P. 1996, *ApJ*, 458, L67
 Bettoni, D., & Galletta, G. 1992, in *Dynamics of Disk Galaxies* (Göteborg: Göteborg University Press), ed. B. Sundelius, 317.
 Carollo, C.M., de Zeeuw, P.T., van der Marel, R.P. Danziger, I.J. & Qian, E.E. 1995, *ApJ*, 441, L25
 de Vaucouleurs, G., de Vaucouleurs, A., Corwin, H. G., Buta, R. J., Paturel, G. & Fouqué, P. 1991, *Third Reference Catalogue of Bright Galaxies* (New York: Springer-Verlag) (RC3)
 Emsellem, E., Pécontal, E., Thiébaud, E., Monnet, G., 1995, 5th Tex-Mex Symposium, Mexico
 Fisher, D. 1994, in *Mass-Transfer Induced Activity in Galaxies*, ed. I. Shlosman (Cambridge: University Press), 349
 Fisher, D., Illingworth, G. & Franx, M. 1994, *AJ*, 107, 160
 Gerhard, O. E. 1993, *MNRAS*, 265, 213
 Kuijken, K. & Merrifield, M. R. 1993, *MNRAS*, 264, 712
 Kuijken, K. & Merrifield, M. R. 1995, *ApJL*, 443, L13
 Kuijken, K. & Tremaine, S. 1992, in *Dynamics of Disk Galaxies* (Göteborg: Göteborg University Press), ed. B. Sundelius, 71.
 Merrifield, M. R. & Kuijken, K. 1994, *ApJ*, 432, 575
 Merrifield, M. R. & Kuijken, K. 1995, *MNRAS*, 274, 933
 Prada, F., Gutierrez, C.M., Peletier, R.F. & McKeith, C.D. 1996, *ApJ*, 463, L9
 Rix, H.-W. & White, S. D. M. 1992, *MNRAS*, 254, 389
 Rix, H.-W., Franx, M., Fisher, D. & Illingworth, G. 1992, *ApJ*, 400, L5
 Roberts, M.S., Hogg, D. E., Bregman, J. N., Forman, W. R., & Jones, C. 1991, *ApJS*, 75, 751
 Rubin, V., Graham, J. & Kenney, J. 1992, *ApJ*, 394, L9
 Saha, P. & Williams, T.B. 1994, *AJ*, 107, 1295
 Sandage, A. & Tammann, G. 1981, *A Revised Shapley-Ames Catalog of Bright Galaxies* (Washington D.C.: Carnegie Institution Pub. 638) (RSA)
 Statler, T.S. 1995, *AJ*, 109, 1371
 Thakar, A.R. & Ryden, B.S. 1996, *ApJ*, 461, 55
 van der Marel, R. P. & Franx, M. 1993, *ApJ*, 407, 525
 van der Marel, R.P., Evans, N.W., Rix, H.-W., White, S.D.M. & de Zeeuw, T. 1994, *MNRAS*, 271, 99
 Whitmore, B.C., Lucas, R.A., McElroy, D.B., Steiman-Cameron, T.Y., & Sackett, P.D. 1990, *AJ*, 100, 1489